Microscopic wrinkles on supported surfactant monolayers

Quan Zhang* and T. A. Witten†
Department of Physics and James Franck Institute, University of Chicago, Chicago, Illinois 60637, USA
(Received 31 July 2007; revised manuscript received 10 October 2007; published 26 October 2007)

We discuss mechanical buckling instabilities of a rigid film under compression interacting repulsively with a substrate through a thin fluid layer. The buckling occurs at a characteristic wavelength that increases as the one-fourth power of the bending stiffness, such as the gravitational instability studied previously by Milner *et al.* However, the potential can affect the characteristic buckling wavelength strongly, as predicted by Huang and Suo. If the potential changes sufficiently sharply with thickness, this instability is continuous, with an amplitude varying as the square root of overpressure. We discuss three forms of interaction important for the case of Langmuir monolayers transferred to a substrate: Casimir–van der Waals interaction, screened charged double-layer interaction, and the Sharma potential. We verify these predictions numerically in the van der Waals case.

DOI: 10.1103/PhysRevE.76.041608 PACS number(s): 46.32.+x

I. INTRODUCTION

The advent of controlled molecular scale films and deposition methods has revealed a number of fine-scale wrinkling instabilities [1–3]. At the same time, several new and general features in the buckling of macroscopic films have been identified [4–6]. Some of these are elaborations of the simple Euler buckling of a compressed rod or sheet [7,8]. Recently, Cerda and Pocivavsek [9] have considered rigid, compressed sheets on the surface of a liquid in the presence of gravity. This extends an earlier treatment of Milner, Joanny, and Pincus [10] adapted to lipid monolayers at an air-water interface. Under these conditions the Euler buckling occurs not at zero wave vector but at a finite wave vector determined by the bending modulus and liquid density. We call this mode of buckling gravity-bending buckling.

Folding structure of laterally compressed surfactant monolayers at the air-water interface is a well-known phenomenon [11,12]. The initial instability leading to these folds may be related to the gravity-bending buckling noted above. The observed folding length scale resembles the predicted wavelength of gravity-bending buckling [9]. Analogous folding has recently been observed in solid nanocrystal monolayers [13].

Additional topographic structure is observed when compressed lipid monolayers are transferred to a solid substrate via the inverted Langmuir-Schaeffer method [14]. These supported monolayers and bilayers are increasingly common in the study of biological membranes [15–19]. The layer thus transferred is positioned for easier study. Initially these transferred layers are separated from the substrate by a cushion of the carrier liquid. Any topographic patterning of these transferred layers can readily be observed [16,20]. Such patterning is likely affected by interaction with the substrate. Likewise, any buckling of a supported monolayer must be affected by the substrate. To study transferred monolayers under the high compressions where buckling is expected seems feasible, though to our knowledge no such studies have been performed.

In this paper we investigate a class of wrinkling instabilities that are generalizations of gravity-bending buckling. These instabilities occur when a deformable surface such as a lipid monolayer lies above a solid substrate on a cushion of fluid. The interaction of the surface with the substrate can then play the role of gravity. This interaction alters the gravity-bending instability in several ways. It makes the unstable wavelengths depend on depth d. These wavelengths generally are much smaller than those predicted by the gravity-bending instability.

In order to investigate the effect of the substrate in its simplest form, our treatment neglects several effects that may be important in practice [21]. In practice, some external forcing on the film is required in order to create the lateral pressure to induce buckling. For example, regions outside the region under study may be bonded to the substrate. In practice the time dependence of the buckling may be important in determining its wavelength. This is especially true in cases where the equilibrium buckling transition is discontinuous. These effects have been extensively explored in the semiconductor film literature [22–24]. Below we shall merely assume that a uniform unixial stress is imposed on the region in question and will only investigate the initial buckling instability as influenced by the substrate interaction. Further, we shall suppose that the buckling film is inextensible. In the Appendix we show that the inextensible approximation is appropriate for the lipid monolayers such as those of Refs. [11,12].

Moreover, the interaction alters the qualitative nature of the instability. The gravity-bending instability is a runaway or subcritical instability at constant surface pressure. Here the amplitude of the wrinkles jumps from zero to a large value determined by other aspects of the system. However, substrate interactions can change this behavior, making the amplitude a continuous function of surface pressure. The criterion for a continuous transition can be stated generally in terms of the second and fourth derivatives of the interaction potential with separation.

In the following sections we discuss the substrate-bending instability in terms of a general interaction potential $\phi(d)$.

*quanz@uchicago.edu
†t-witten@uchicago.edu

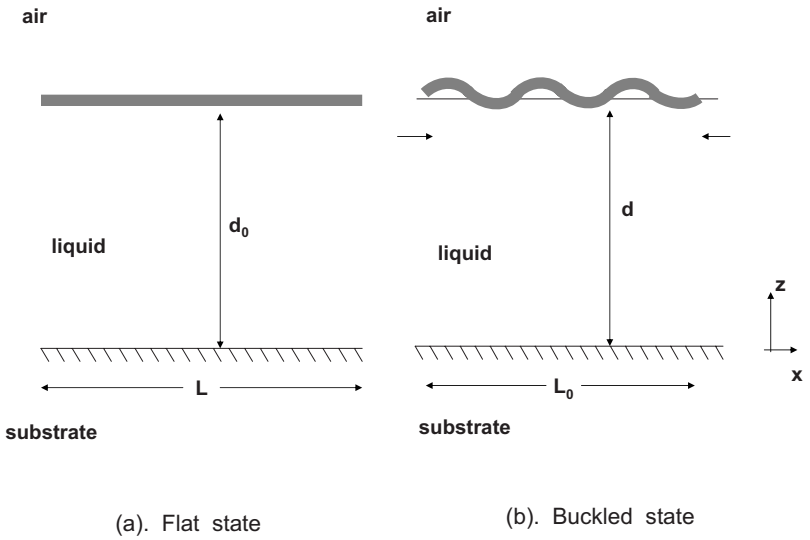

FIG. 1. One-dimensional model used in the theory. The y axis is pointing out of the figure. (a) Initial flat state with no compression. (b) Buckled state with large enough compression.

We determine the unstable wavelength and the condition for a continuous transition. In the following section we consider three specific potentials commonly encountered in liquid films. The first is the Casimir–van der Waals interaction, $\phi(d)=A/(12\pi d^2)$. The second is the screened charged double-layer interaction common in aqueous films with charged interfaces. The third is the Sharma potential used to describe molecularly thin water films. All of these potentials produce continuous wrinkling for sufficiently thick films. We conclude that this substrate-bending buckling should be readily observable.

II. THEORY OF WRINKLING INSTABILITY

A. Wavelength of microscopic wrinkles

In the analysis below, we will consider a simplified model of a Langmuir monolayer. Suppose an insoluble surfactant layer is sitting at the interface between air and a liquid subphase. The elastic property of a layer, with finite thickness t, is characterized by the bending modulus B [25],

$$B = \frac{Et^3}{12(1-\nu^2)}, \tag{1}$$

where E is Young's modulus and ν is the Poisson ratio in the continuum theory. A solid substrate is placed under the subphase, as shown in Fig. 1. Interaction between the solid substrate and liquid subphase takes the form of a substrate potential $\phi(d)$ [26]. For different interactions, the functional forms of $\phi(d)$ are different [27]. For example, if the interaction is of pure van der Waals type, we have

$$\phi(d) = \frac{A}{12\pi d^2}, \tag{2}$$

where A is the Hamaker constant [26]. It can take positive or negative values depending on properties of substrate and subphase. Possible retardation effects are not considered in this paper. In a Langmuir trough, one can compress the surfactant layer with external pressure Π_{ex}. Elastic strain energy is stored in the elastic layer upon compression. It is expected that if Π_{ex} exceeds some critical value Π_c, the elastic layer will enter a buckled state and relax the strain energy in a third dimension, similar to the Euler buckling of a rod. We recall that the critical pressure Π_c is independent of the compressibility of the layer, although the corresponding strain depends on the compressibility [7]. In the following analysis a constant external pressure Π_{ex} is exerted on the Langmuir monolayer. A buckling transition is induced by displacing the boundary. In the wrinkled state, total area S of the surfactant layer is

$$S = \int_{S_0} [1 + (\nabla \xi)^2]^{1/2} ds. \tag{3}$$

The above integral is taken over the projected area S_0 on the horizontal x-y plane and ds is a surface element in S_0. The quantity $\xi(x,y)$ is the vertical displacement of interface from a flat state. The height profile of the interface is $d(x,y)=d_0+\xi(x,y)$, where d_0 is the height of a flat state with no surface deformation. We assume that no subphase fluid enters or leaves, so that the volume of subphase under the initial flat surface is fixed during deformation,

$$\int_{S_0} \xi(x,y) ds = 0. \tag{4}$$

Another parameter needed is the surface density of surfactant, $\sigma=N/S$, where N is the total number of surfactant molecules. For constant external pressure Π_{ex}, the Gibbs free energy is written as [10,28]

$$G = \gamma_0(S - S_0) + F_l + F_b + F_i + \Pi_{ex} S_0, \tag{5}$$

where γ_0 is the surface tension of a free interface without any compression. The first term denotes the change in interfacial energy. F_l is the surfactant free energy. It is related to

σ via the relation $F_l = Sf_l(\sigma)$. The last term is an analogy of the pressure P times volume V term in the Gibbs free energy of a conventional gas. F_b and F_i are bending energy and substrate potential energy, respectively. For small surface deformation ($|\xi/d_0| \ll 1$), the bending energy F_b is given by the Helfrich energy [29,30],

$$F_b = \frac{B}{2}\int_{\text{material surface}} (C - C_0)^2 = \frac{B}{2}\int_{S_0} (C - C_0)^2 [1 + (\nabla\xi)^2]^{1/2} ds, \tag{6}$$

where $C(x,y)$ is the mean curvature of the interface and C_0 is the spontaneous curvature of surfactant layer. Again we have expressed the integral in terms of the projected area as in Eq. (3). C_0 has no effect on the following analysis and we shall neglect it henceforth [28]. The substrate potential energy is

$$F_i = \int_{S_0} \phi(d)[1 + (\nabla\xi)^2]^{1/2} ds - \phi(d_0)S, \tag{7}$$

where the initial flat state is chosen as a reference state for the potential energy. Our treatment can be simplified by supposing that the film is *inextensible*, as justified in the Appendix. In that case, the molecular density σ is fixed and the energy F_l is a mere constant. Then for different values of external pressure Π_{ex}, the equilibrium configuration of the system is obtained by minimizing the Gibbs free energy with the inextensibility constraint of the surfactant layer, S =const. Introducing a Lagrange multiplier θ to incorporate this constraint, the functional that we need to minimize is

$$G' = G - \theta\left(S - \int_{S_0} [1 + (\nabla\xi)^2]^{1/2} ds\right). \tag{8}$$

In the rest of this paper, we assume that relaxation of strain energy only occurs in the x direction, as shown in Fig. 1. In the y direction, the system has translational invariance. As a result, we may minimize the Gibbs free energy per unit length in the y direction, which we denote as g',

$$g' = g - \theta\left(L - \int_{L_0} [1 + (\dot{\xi})^2]^{1/2} dx\right) = \gamma_0(L - L_0) + Lf_l(\sigma) + f_b + f_i + \Pi_{ex}L_0 - \theta\left(L - \int_{L_0} [1 + (\dot{\xi})^2]^{1/2} dx\right), \tag{9}$$

where L is the total length of surfactant layer and L_0 is the projected length in the x direction, as shown in Fig. 1. In the above expression, $\dot{\xi}$ denotes the derivative of ξ with respect to the x coordinate. In the one-dimensional model, the mean curvature C is given by

$$C = \ddot{\xi}(1 + \dot{\xi}^2)^{-3/2}. \tag{10}$$

Using this expression, the bending free energy (per unit length in the y direction) f_b and its expansion in small deformation approximation take the form

$$f_b = \frac{B}{2}\int_{L_0} (\ddot{\xi})^2 (1 + \dot{\xi}^2)^{-5/2} dx \sim \frac{B}{2}\int_{L_0} (\ddot{\xi})^2 \left(1 - \frac{5}{2}\dot{\xi}^2 + \frac{35}{8}\dot{\xi}^4 - \cdots\right) dx. \tag{11}$$

Similarly, the substrate potential energy f_i and its expansion take the form

$$f_i = \int_{L_0} \phi(d)(1 + \dot{\xi}^2)^{1/2} dx - \phi(d_0)L \sim \int_{L_0} dx \left(\phi(d_0) + \phi'(d_0)\xi + \frac{\phi^{(2)}(d_0)}{2}\xi^2 + \frac{\phi(d_0)}{2}\dot{\xi}^2 + \frac{\phi^{(3)}(d_0)}{6}\xi^3 + \frac{\phi'(d_0)}{2}\xi\dot{\xi}^2 + \frac{\phi^{(4)}(d_0)}{24}\xi^4 + \frac{\phi^{(2)}(d_0)}{4}\xi^2\dot{\xi}^2 - \frac{\phi(d_0)}{8}\dot{\xi}^4 + \cdots\right) - \phi(d_0)L. \tag{12}$$

Here $\phi'(d_0), \phi^{(2)}(d_0), \ldots$ denote the derivatives of ϕ with respect to the z coordinate and are evaluated in the flat state. Integration of the first-order term in ξ vanishes because of volume conservation, Eq. (4). Furthermore, we will choose the origin of the x coordinate such that integration ranges from $-L_0/2$ to $L_0/2$. Different coordinate systems differ only in small boundary terms, which are negligible if the system is large enough. In the following discussion it will be clear in what sense we mean by large enough. Minimizing g' with respect to L_0, L and surface undulation $\xi(x)$ and keeping only the lowest order terms in ξ, we obtain the following equilibrium equations of state [10]:

$$\Pi_{ex} - \gamma_0 + \phi(d_0) + \theta = 0, \tag{13}$$

$$\gamma_0 - \phi(d_0) + \theta + \frac{\partial[Lf_l(\sigma)]}{\partial(L)} = 0, \tag{14}$$

$$B\frac{d^4\xi}{dx^4} - [\theta + \phi(d_0)]\ddot{\xi} + \phi^{(2)}(d_0)\xi = 0. \tag{15}$$

The Lagrange multiplier θ is related to the external pressure Π_{ex}, $\theta = \gamma_0 - \Pi_{ex} - \phi(d_0)$. Moreover, the equilibrium shape of the interface $\xi(x)$ must satisfy the above differential equation. Using an *Ansatz* of sinusoidal deformation, $\xi(x) = h\sin(qx)$, where h is the amplitude and q is the wave number, we obtain

$$Bq^4 + (\gamma_0 - \Pi_{ex})q^2 + \phi^{(2)}(d_0) = 0, \tag{16}$$

where $\theta = \gamma_0 - \Pi_{ex} - \phi(d_0)$ has been used [by Eq. (13)]. We have the following relation between external pressure Π_{ex} and wave number q:

$$\Pi_{ex} - \gamma_0 = Bq^2 + \frac{\phi^{(2)}(d_0)}{q^2}. \tag{17}$$

An equivalent equation was obtained by Huang *et al.* [31]. Minimizing the right-hand side of Eq. (17) with respect to q,

we obtain the smallest external pressure Π_c for buckling instability and critical wave number q_c,

$$q_c = \left(\frac{\phi^{(2)}(d_0)}{B}\right)^{1/4},$$

$$\lambda_c = 2\pi[B/\phi^{(2)}(d_0)]^{1/4},$$

$$\Pi_c = \gamma_0 + 2[B\phi^{(2)}(d_0)]^{1/2}. \tag{18}$$

If the gravitational energy of a liquid subphase (in air) is considered, we may choose the flat state as reference and take $\phi(d)=\rho g\xi^2/2$. The threshold external pressure Π_c and critical wave number q_c in this particular case are

$$\Pi_c = \gamma_0 + 2(B\rho g)^{1/2},$$

$$q_c = \left(\frac{\rho g}{B}\right)^{1/4}. \tag{19}$$

The results in Eq. (19) were obtained by Milner *et al.* in Ref. [10]. Gravitational energy is important in macroscopic scale with relatively thick liquid subphase. However, in microscopic scale ($d<100$ nm), different types of substrate interaction between solid substrate and liquid subphase, e.g., van der Waals interaction, become dominant, while gravity is negligible. The buckling transition now leads to microscopic wrinkles. Our result in Eq. (18) is a generalization to this microscopic range. The effect of different types of interaction will be discussed in a later section.

B. Second-order buckling transition

In the preceding section, we used the small deformation approximation and expanded the Gibbs free energy to the lowest order in surface displacement $\xi(x)$. A relation between external pressure Π_{ex} and wave number q of wrinkles is obtained in Eq. (17). In order to study the undulation amplitude h and possible order of the buckling transition, higher order terms in the expansion should be included in the analysis. We are particularly interested in finding out the existence conditions for a continuous, second-order transition. From Landau's classical theory of phase transition [32], a first-order (discontinuous) transition will occur if the coefficient of the fourth-order term of free-energy expansion with respect to the order parameter [$\xi(x)$ in our case] is negative. In this section, we will include terms up to the fourth order of ξ. The inextensibility constraint of the surfactant layer yields

$$L = \int_{L_0} (1+\dot{\xi}^2)^{1/2} dx = \text{const}. \tag{20}$$

Under the inextensibility constraint (20), we can drop constant terms in expression (9) and minimize with respect to the following functional of L_0 and $\xi(x)$:

$$g_1 = (\Pi_{ex} - \gamma_0)L_0 + f_b + f_i + \phi(d_0)L. \tag{21}$$

The projected length L_0 in the x direction and the surface deformation $\xi(x)$ are not independent variables. They are related through the constraint (20). Assuming sinusoidal deformation, $\xi(x)=h\sin(qx)$, it leads to an expression of L_0 in terms of L, h, and q. We will revisit the assumption of incompressibility in Sec. V. Inserting this expression for L_0 into Eq. (21), we see that the functional g_1 has the form of Landau free-energy expansion [32]. First, we compute the expression for L_0. Expanded to the fourth order in $\xi(x)$, i.e., $h\sin(qx)$, the constraint (20) is

$$L = \int_{-L_0/2}^{L_0/2} dx(1+\dot{\xi}^2)^{1/2} \sim \int_{-L_0/2}^{L_0/2} dx\left(1+\frac{1}{2}\dot{\xi}^2 - \frac{1}{8}\dot{\xi}^4\right)$$
$$\sim L_0\left(1+\frac{1}{4}h^2q^2 - \frac{3}{64}h^4q^4\right). \tag{22}$$

In the last step, we keep only extensive terms, proportional to the size of the system L_0, and neglect boundary terms. The boundary terms are of the order of a wavelength of wrinkles $2\pi/q$. The approximation made in Eq. (22) is thus essentially that the wavelength of wrinkles is much smaller than the dimension of Langmuir system in the x direction, $|qL| \gg 1$. If this condition is satisfied, the approximation (22) is valid and we obtain the following expression for the projected length L_0:

$$L_0 = L\left(1+\frac{1}{4}\tilde{h}^2 - \frac{3}{64}\tilde{h}^4\right) \sim L\left(1-\frac{1}{4}\tilde{h}^2 + \frac{7}{64}\tilde{h}^4\right), \tag{23}$$

where the slope amplitude $\tilde{h}=hq$ is a dimensionless parameter and $|\tilde{h}| \ll 1$ in the small deformation approximation. Similarly, expanding the functional g_1 in Eq. (21) to the fourth order in ξ and neglecting boundary terms, we obtain

$$g_1 \sim L_0\left[-\theta + \frac{\tilde{h}^2}{4}\left(Bq^2 + \phi(d_0) + \frac{\phi^{(2)}(d_0)}{q^2}\right)\right.$$
$$\left. + \frac{\tilde{h}^4}{64}\left(-10Bq^2 - 3\phi(d_0) + \frac{2\phi^{(2)}(d_0)}{q^2} + \frac{\phi^{(4)}(d_0)}{q^4}\right)\right], \tag{24}$$

where $\theta=\gamma_0-\Pi_{ex}-\phi(d_0)$ is the Lagrange multiplier defined in the preceding section. g_1 depends on the dimensionless variable $\tilde{h}$ and wave number q. Using the expression of L_0 in Eq. (23),

$$g_2 \equiv g_1/L \sim -\theta + \frac{\tilde{h}^2}{4}\left(Bq^2 + \theta + \phi(d_0) + \frac{\phi^{(2)}(d_0)}{q^2}\right)$$
$$+ \frac{\tilde{h}^4}{64}\left(\frac{\phi^{(4)}(d_0)}{q^4} - \frac{2\phi^{(2)}(d_0)}{q^2} - 7\theta - 7\phi(d_0) - 14Bq^2\right). \tag{25}$$

The equilibrium configuration minimizes the value of g_2. In the above expression $g_2 \to -\infty$ as $q \to \infty$. It seems that the minimum value of g_2 does not exist. This paradox is solved by noticing that the value of wave number q cannot vary arbitrarily. In the small deformation approximation, we have assumed that $\tilde{h}=hq$ is a small quantity. As a result, q cannot be arbitrarily large. Furthermore, q should be close to its critical value q_c near transition,

$$q = q_c(1 + \delta), \tag{26}$$

where δ is a small dimensionless parameter and $\delta > 0$ if wave number q is a continuous function of compression. Using the expression (26) for q and keeping the terms up to the second order in δ, we obtain

$$g_2 \sim -\theta + A_1\tilde{h}^2 + A_2\tilde{h}^4, \tag{27}$$

where the coefficients A_1 and A_2 are quadratic functions of δ,

$$A_1 = \frac{1}{4}(\Pi_c - \Pi_{ex}) + \delta^2\pi, \tag{28}$$

$$A_2 = \frac{1}{64}[a - 16b - 7\theta - 7\phi(d_0)] + \frac{\delta}{16}(-a - 6b) + \frac{\delta^2}{32}(5a - 10b), \tag{29}$$

where the two parameters b and a are defined as

$$a \equiv [B\phi^{(4)}(d_0)]/\phi^{(2)}(d_0),$$

$$b \equiv [B\phi^{(2)}(d_0)]^{1/2}. \tag{30}$$

The minimum value of g_2 exists for some positive x and δ, only if the coefficients A_1 and A_2 satisfy the inequalities

$$A_1 < 0, \quad A_2 > 0. \tag{31}$$

Furthermore, if inequalities (31) are true, g_2 can achieve its minimum at $\tilde{h}_{min}$ and δ_{min},

$$\tilde{h}_{min} = D_{\tilde{h}}(\Pi_{ex} - \Pi_c)^{1/2},$$

$$\delta_{min} = D_\delta(\Pi_{ex} - \Pi_c), \tag{32}$$

where $D_{\tilde{h}}$ and D_δ are some positive coefficients. Obviously, $\tilde{h}_{min}$ and δ_{min} are positive when $\Pi_{ex} > \Pi_c$ and approach zero, as the external pressure Π_{ex} approaches its threshold value Π_c from above. In other words, the values of $\tilde{h}_{min}$ and δ_{min} can be made arbitrarily small by approaching the transition point. As a result, the terms involving δ in A_1 and A_2 are of higher order and can be neglected in comparison with the finite constant term. The inequalities (31) are reduced to

$$\Pi_c - \Pi_{ex} < 0, \tag{33}$$

$$a - 16b - 7\theta - 7\phi(d_0) > 0. \tag{34}$$

The first inequality will be true if $\Pi_{ex} > \Pi_c$. Using the expression of γ, a, and b, we can rewrite the second inequality as

$$[B\phi^{(4)}(d_0)]/\phi^{(2)}(d_0) - 2[B\phi^{(2)}(d_0)]^{1/2} > 7(\Pi_c - \Pi_{ex}). \tag{35}$$

Since the right-hand side approaches zero from below as Π_{ex} decreases to Π_c, we get the condition

$$\phi^{(4)}(d_0) > 2\left(\frac{\phi^{(2)}(d_0)^3}{B}\right)^{1/2}, \tag{36}$$

where we have used the expression (18) for q_c. In order to have a second-order buckling transition, the inequality (36) is the condition that must be satisfied by the substrate potential $\phi(d)$. The above criterion for the order of buckling transition does not change after including the second harmonic term $\alpha h \sin(2qx)$. Because α does not affect A_1 and enters A_2 as $\alpha^2\tilde{h}^2$, the second harmonic term affects g_2 only at order $\tilde{h}^6$ or higher. As a result, it does not change the criterion in inequality (36). In the case of gravitational potential energy of liquid subphase, $\phi(d) = \rho g \xi^2/2$, we have $\phi^{(2)}(d_0) = \rho g > 0$ and $\phi^{(4)}(d_0) = 0$. The relation (36) cannot be satisfied. Therefore, we will have a first-order buckling transition in this case [10]. However, the relation (36) may be satisfied for some types of substrate potentials. We will discuss its explicit forms in the next section and consider the possibility of a second-order buckling transition for different types of interaction. Although our conditions are necessary for a continuous transition, they are not completely sufficient. To show that no discontinuous transition occurs, we would have to show that *no* displacement $\xi(x)$ has a $\Pi_{min} < \Pi_c$. We considered only small and harmonic $\xi(x)$.

III. EXAMPLE POTENTIALS

In this section, we will consider some examples of substrate potentials and find out the corresponding existence conditions for the second-order buckling transition.

A. Nonretarded van der Waals interaction

Nonretarded van der Waals interaction between liquid subphase and solid substrate takes the form [26]

$$\phi(d) = \frac{A}{12\pi d^2}. \tag{37}$$

Here A is the Hamaker constant and has the dimension of energy. It can be positive or negative depending on the properties of liquid subphase and solid substrate. If A is positive, van der Waals interaction leads to an effective repulsion between liquid-air and liquid-substrate interfaces and favors a thicker liquid film, i.e., larger d. On the other hand, if $A < 0$, the liquid film can be unstable. Spontaneous fluctuations may rupture the liquid film via spinodal dewetting [33]. The value of A is typically in the range of 10^{-20} J to 10^{-19} J [26]. From Eq. (18), we have the critical wave number q_c and wavelength λ_c,

$$q_c = \frac{1}{d_0}\left(\frac{A}{2\pi B}\right)^{1/4},$$

$$\lambda_c = 2\pi d_0\left(\frac{2\pi B}{A}\right)^{1/4}. \tag{38}$$

Thus q_c and λ_c exist only in the case $A > 0$, i.e., for stable liquid subphase. The second-order buckling transition requirement (36) reduces to

$$A < 200\pi B, \tag{39}$$

which does not depend on the thickness of the liquid subphase d_0. This independence of thickness can be understood by noticing that as we increase the thickness of liquid subphase d_0, van der Waals potential energy density decreases as A/d_0^2. Meanwhile, the local curvature of surfactant layer C is of the order of $1/d_0$, so bending free energy density varies as B/d_0^2, which has the same functional form as van der Waals interaction. As a result, we expect the criterion does not depend on the thickness of the liquid subphase d_0 and is a relation between the Hamaker constant A and bending modulus B. As long as A and B satisfy condition (39), microscopic wrinkles can be formed through a second-order buckling transition. For a lipid monolayer $B \gtrsim 10kT$ [34], which is 4×10^{-20} J at 25 centigrade. The smallest λ_c compatible with Eq. (39) is

$$\lambda_{c\,\min} = 2\pi d_0/\sqrt{10} \approx 2.0 d_0. \tag{40}$$

The wavelength λ_c increases only gradually from the minimum because of the weak dependence on B/A in Eq. (38). For practical purposes, the buckling wavelength is confined to scales of order d_0. In the microscopic range that we are discussing, $d_0 < 100$ nm. Typically, the dimension of the Langmuir system L in the horizontal direction is about 1 mm, so the condition of a large enough system $|q_c L| \gg 1$ is satisfied.

B. Charged double-layer interaction

The charged double-layer interaction has the form [27]

$$\phi(d) = \phi_0 \exp(-\kappa d), \tag{41}$$

where $1/\kappa$ is the Debye screening length. The coefficient ϕ_0 is a constant depending on zeta potentials of two surfaces and electrolyte concentration in between. For a 1:1 electrolyte, ϕ_0 can be written as

$$\phi_0 = \frac{64kT\gamma_1\gamma_2 C_s}{\kappa}. \tag{42}$$

In Eq. (42), T is the temperature and C_s is the concentration of electrolyte in the bulk. Moreover γ_i $(i=1,2)$ is related to zeta potentials ζ_{0i} of the two surfaces [27],

$$\gamma_i = \tanh(e\zeta_{0i}/4kT). \tag{43}$$

The potential ϕ_0 is positive if two electrical surfaces have charges of the same sign and repel each other. In the case ϕ_0 is negative, two electrical surfaces attract each other; this may rupture the liquid film via unstable modes of undulation. The above equation is valid in the weak overlap approximation, in which the overlap between electrical double layers is small [35],

$$\kappa d > 1. \tag{44}$$

From Eq. (18), we have the critical wave number q_c and wavelength λ_c,

$$q_c = \left(\frac{\kappa^2\phi_0}{B}\exp(-\kappa d_0)\right)^{1/4},$$

$$\lambda_c = 2\pi\left(\frac{B}{\kappa^2\phi_0}\exp(\kappa d_0)\right)^{1/4}. \tag{45}$$

Thus λ_c and q_c exist only in the case $\phi_0 > 0$, i.e., for stable liquid subphase. The second-order buckling transition condition (36) takes the form

$$d_0 > \frac{1}{\kappa}\ln\left(\frac{4\phi_0}{\kappa^2 B}\right). \tag{46}$$

The smallest λ_c compatible with condition (46) is

$$\lambda_{c\,\min} = 2\sqrt{2}\pi\kappa^{-1}. \tag{47}$$

It is on the order of the Debye screening length κ^{-1}. The wavelength λ_c is an increasing function of d_0. For example, we consider a negatively charged mica substrate and a negatively charged conventional liposome (lecithin/cholesterol 6:4 molar ratio). As an electrolyte, we consider NaCl at concentration $C_s = 0.001$ mol/l. In this case, the Debye screening length is $\kappa^{-1} \approx 10$ nm [27]. At pH 5.8, the zeta potentials of mica surface [36] and conventional liposomes are [37]

$$\zeta_{0\mathrm{mic}} = -104\mathrm{mV} \quad \text{and} \quad \zeta_{0\ \mathrm{lip}} = -20\mathrm{mV}. \tag{48}$$

The value of ϕ_0 is calculated as

$$\phi_0 \approx 2.2 \times 10^{-4}\ (\mathrm{J/m^2}). \tag{49}$$

By the estimation of the bending modulus $B \gtrsim 10kT$ [34], the condition (46) reduces to

$$d_0 > 8.1\ \mathrm{nm}. \tag{50}$$

C. Sharma potential

The Sharma potential is used widely in studies of wetting phenomena between different liquid thin films and solid substrates [38–40], e.g., water on mica. It includes both the apolar (Lifshitz–van der Waals) and polar interactions and has the form

$$\phi(d) = S^{AP}\left(\frac{d_c^2}{d^2}\right) + S^P \exp\left(\frac{d_c - d}{l}\right), \tag{51}$$

where S^{AP} and S^P are apolar and polar contributions to the spreading coefficient. l is the correlation length for polar liquid, and d_c is the Born repulsion cutoff length [38]. In this case, the critical wave number q_c and wavelength λ_c have the form

$$q_c = \frac{1}{d_0 B^{1/4}}\left(6S^{AP}d_c^2 + \frac{S^P d_0^4}{l^2}\exp[(d_c - d_0)/l]\right)^{1/4},$$

$$\lambda_c = 2\pi d_0 B^{1/4}\left(6S^{AP}d_c^2 + \frac{S^P d_0^4}{l^2}\exp[(d_c - d_0)/l]\right)^{-1/4}. \tag{52}$$

The existence requirement of the second-order buckling transition yields

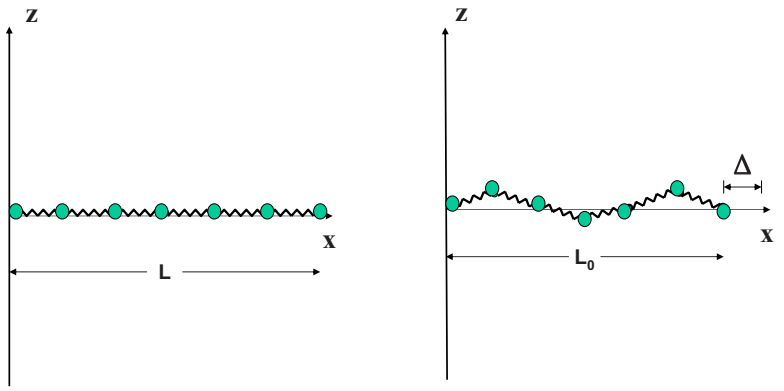

FIG. 2. (Color online) Discrete model of one-dimensional chain of springs used in the simulation. (a) Flat state with no compression. (b) Buckled state with large enough compression.

$$120S^{AP}d_c^2l^4 > -S^P d_0^6 \exp\left(\frac{d_c-d_0}{l}\right) + 2l/\sqrt{B}\left[6S^{AP}d_c^2l^2 + d_0^4 S^P \exp\left(\frac{d_c-d_0}{l}\right)\right]^{3/2}. \tag{53}$$

For example, we consider a lipid monolayer, with bending modulus $B \gtrsim 10kT$, sitting on top of water with a mica substrate below. The numerical values of coefficients are $S^{AP}=20$ mN/m, $S^P=48$ mN/m, $l=0.6$ nm, and $d_c=0.158$ nm [39]. The wavelength λ_c is an increasing function of d_0. In the microscopic range, where the thickness of water subphase $d_0<100$ nm, we obtain an upper bound for λ_c,

$$\lambda_c \lesssim 1.2 \ \mu\text{m}. \tag{54}$$

Obviously, the condition $|q_cL| \gg 1$ is guaranteed. Furthermore, the inequality (53) is true for any positive value of d_0. In other words, the buckling transition will always be second order if the Sharma potential correctly describes the interaction between water subphase and a mica substrate. The following dimensionless quantity changes very slowly with the value of d_0:

$$\eta \equiv B^{1/4}\left(6S^{AP}d_c^2 + \frac{S^P d_0^4}{l^2}\exp[(d_c-d_0)/l]\right)^{-1/4}. \tag{55}$$

In the range of d_0 between 1 nm and 100 nm, $\eta \in [0.8, 1.9]$. Thus, the critical wavelength λ_c can be written as

$$\lambda_c = 2\pi d_0 \eta \gtrsim 5.0 d_0. \tag{56}$$

For the estimation in the last step, η takes the smallest value 0.8 in this range.

IV. NUMERICAL RESULTS

In order to verify our results and explore the predicted wrinkling phenomena concretely, we have done a discrete numerical implementation of the system. The numerical simulation was carried out using the MATHEMATICA program. We modeled the surfactant layer by a one-dimensional chain of nodes connected by springs with unstretched length a and spring constant k. The unstretched length a is set to be 1 in the simulation for convenience. In order to impose the inextensibility constraint, we set the spring constant k to be a very large value. A bending energy of $B\theta_{i,(i+1)}^2/2$ is assigned to every pair of adjacent springs, where $\theta_{i,(i+1)}$ is the angle between these two springs along the chain direction. The total bending energy f_b is a sum of all pairs along the chain. In the numerical simulation we set the free liquid-air surface tension in our theory $\gamma_0=0$. The substrate potential is discretized correspondingly by replacing the integral with a summation along the chain. With no compression the chain adopts a flat configuration lying on the x axis. In the simulation, the first node is fixed at the origin. In order to reduce the influence of boundary effects in a finite system used in the simulation, we fix the z coordinate of the last node to be zero, while its x coordinate was determined by the amount of compression Δ, as shown in Fig. 2. All the other nodes are movable both in x and z directions in the process of minimization. The total free energy g^* of this discrete model takes the form

$$g^* = \Pi_{\text{ex}}L_0 + f_b + f_i + f_k = \Pi_{\text{ex}}L_0 + g_1^*, \tag{57}$$

where f_b, f_i, and f_k are bending energy, substrate potential energy, and elastic energy stored in the springs. The quantity g_1^* is the sum of these. For the flat reference state, the above three energy terms are zero. So the total free energy for the flat state is

$$g^* = \Pi_{\text{ex}}L, \tag{58}$$

where L is the total length of the chain. The compression is $\Delta = L - L_0$. At each fixed amount of compression Δ, we minimized the value of $g_1^*(\Delta)$ and computed the smallest external pressure $\Pi_{\text{min}}(\Delta)$ needed to reach this compression via the following equation:

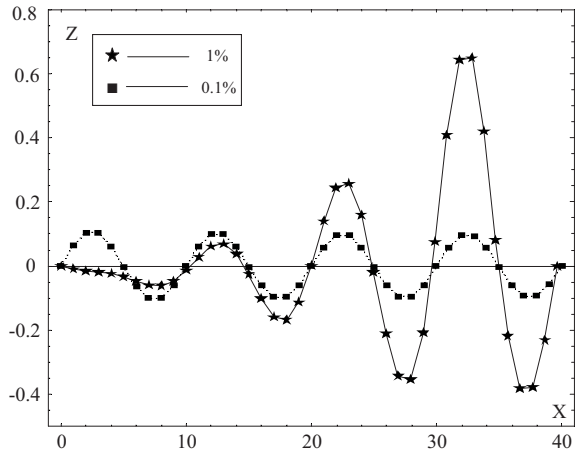

FIG. 3. Configurations with 41 nodes as compression Δ changes. The box in the graph shows the amount of compression. van der Waals interaction is used in this simulation. Parameter values, $A=200$, $B=1$, $d_0=3.780\,36$, $k=10^{11}$. The predicted wavelength of wrinkling, $\lambda_c=10$. The nonuniformity of the amplitude with 1% compression is due to nonlinear effects approaching a possible wrinkle-to-fold transition [9]. The position of a fold could change for different initial conditions of minimization.

$$\Pi_{\min}(\Delta) = \frac{g^*_{1\ \min}(\Delta)}{\Delta}. \tag{59}$$

We chose a value of d_0 such that the predicted λ_c was commensurate with the system, namely $\lambda_c=10$. Then starting from a finite amount of compression, e.g., $\Delta=1\%$, we gradually lowered the value of Δ. If our theory is correct, the chain will approach a sinusoidal shape with wavelength λ_c. Moreover $\Pi_{\min}(\Delta)$ should approach Π_c as Δ goes to zero. The order of buckling transition can be deduced from the functional shape of $\Pi_{\min}(\Delta)$. For a second-order or continuous transition, $\Pi_{\min}(\Delta)$ is a monotonic increasing function of Δ. There is no jump when crossing the transition point. In the case of a first-order transition, $\Pi_{\min}(\Delta)$ is not monotonic. It has a minimal value $\Pi^*_{\min}$ at a nonzero compression Δ^*. As a result, as soon as Π_{ex} exceeds $\Pi^*_{\min}$, the configuration will jump to this finite amount of compression showing the property of a first-order buckling.

A typical sequence of chain configurations with 41 nodes as we changed the amount of compression is shown in Figs. 3 and 4. Figure 5 shows the agreement between predicted values of Π_c and $\Pi_{\min}$ from the simulation for several cases. It is noticed that Π_c is a constant function of A, if the buckling wavelength λ_c is fixed.

Verifying the predicted transition from continuous to discontinuous wrinkling proved to be more subtle. Even though the ratio A/B is nearly a factor of 2 above the predicted threshold, we did not see any evidence of discontinuous buckling using the discrete model. To understand this required a second numerical method. As we discuss below, it reveals that the discontinuity is too weak to have been seen in the discrete model.

The second numerical method is based on a continuous model. To simplify the calculation, we took a single sinusoidal mode as *Ansatz*, $h\sin(qx)$. For convenience, only one period of wrinkling is included in the continuous model, while a real system is composed of many copies of it. The wavelength λ changes as we change the amount of compression Δ, $\lambda=\lambda_c-\Delta$. Using a similar approach as the discrete model described above, we can compute $\Pi_{\min}(\Delta)$ for each amount of compression. The order of transition is still determined by the functional shape of $\Pi_{\min}(\Delta)$. This time not only the values of Π_c but also the order of buckling are in good agreement with our theoretical prediction. The paradox with the discrete model is also explained. As it is shown in Fig. 6, the first-order transition is very weak in the case of van der Waals interaction. With $A/B=1000$, $\Pi_{\min}$ has a minimal value at 1% compression with a 0.6% change in $\Pi_{\min}$. Thus the buckling transition is first order. However, such a small change in $\Pi_{\min}$ cannot be detected in the above discrete model. Based on the above numerical results, our theory makes good prediction for the substrate-induced buckling transition.

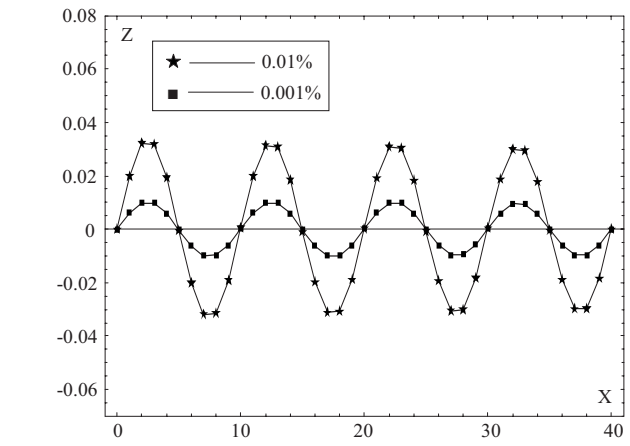

FIG. 4. Configurations with 41 nodes as compression Δ changes. The box in the graph shows the amount of compression. Parameter values are the same as in Fig. 3.

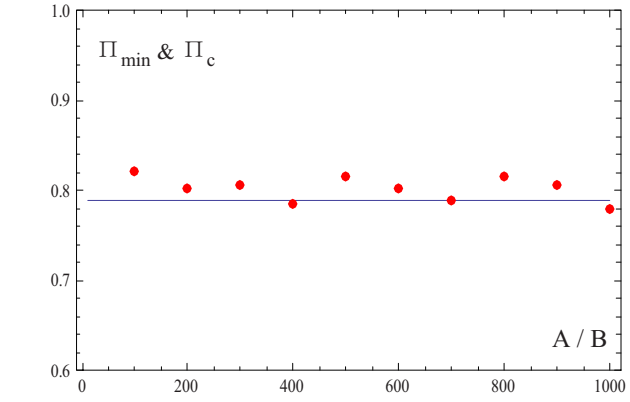

FIG. 5. (Color online) Theoretically predicted Π_c and $\Pi_{\min}$ from simulation as functions of ratio A/B. B is fixed at 1. Solid line represents prediction from theory. Discrete points are values of $\Pi_{\min}$ from the simulation.

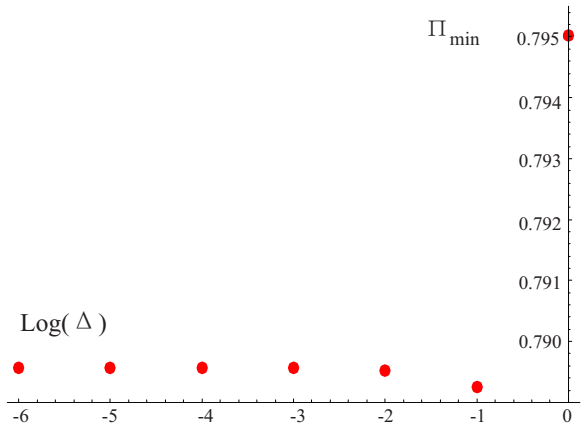

FIG. 6. (Color online) $\Pi_{\min}$ versus $\ln(\Delta)$ for very weak first-order transition in the case of van der Waals interaction, $A=1000$, $B=1$, $d_0=5.652\,95$. The critical wavelength is $\lambda_c=10$.

V. DISCUSSION

In the preceding sections, a substrate-bending model was constructed. Here we discuss the implications of this model. Using our model, we have made a prediction about wrinkling wavelength λ_c with large enough compression $\Pi_{ex}>\Pi_c$ and the order of buckling transition. In order for our mechanism to account for wavelengths of hundreds of nanometers, the trapped fluid layer itself would have to be many nanometers thick. During the transfer of a monolayer to substrate, such thick fluid layers usually exist. The compressive stress required to buckle the surfactant layer could be developed during this transfer and rapid drying after deposition.

The wrinkling mechanism predicted here is expected in any supported monolayer or bilayer system with sufficient compression. A well-defined wrinkling wavelength λ_c is given in terms of the thickness of the subphase d_0, the bending modulus of the surfactant layer B, and functional form of the substrate potential $\phi(d)$. Information about these microscopic variables is embedded in the experimentally observed wavelength. It is especially useful if one can control the external pressure Π_{ex}. The properties of gravitational wrinkles have been experimentally studied [9]. Gravitational buckling appears to give rise to a strongly first-order wrinkling-to-folding transition, which contrasts with our very weak first-order transition in the case of van der Waals interaction. Some other forms of substrate potential $\phi(d)$ may give rise to a stronger first-order transition.

These surfactant layers are potentially subject to another kind of instability different from the extensive wrinkling investigated here. The boundary conditions may be such that the boundary region buckles while the bulk of the layer is still in a stable state. These boundary induced deformations of surfactant layers have been studied [41,42]. Such boundary buckling was an important factor in our discrete simulation. It prevented us from studying arbitrary wavelengths. Also our methods only allowed us to study the region of incipient instability. There may be interesting phenomena analogous to the gravitational wrinkling-to-folding transition that we have missed.

Inextensibility of the surfactant layer is an important assumption in our theory. If this constraint were released, the system would have a compression mode as an extra degree of freedom to store elastic energy besides the bending mode studied above. As shown in the Appendix, in the limit of small deformation approximation, finite compressibility influences only fourth order and higher terms in the free energy, so it does not change the expressions of the threshold external pressure Π_c and the critical wavelength λ_c. Moreover, if the system were not too far away from the transition threshold between first-order buckling and second-order buckling, the inextensibility would be a good approximation in the experiments of interest here.

VI. CONCLUSION

As supported monolayers and bilayers become more commonly studied, we expect that the type of wrinkling predicted here will be observed and used to infer local properties, such as substrate depth, bending modulus of surfactant layer, etc. It will be of interest to see how such buckling occurs in time, and what counterparts of the wrinkling-to-folding transition might exist.

ACKNOWLEDGMENTS

The authors would like to thank Professor Ka Yee Lee and her group members, Guohui Wu and Shelli Frey, for providing experimental data. The authors also want to thank Luka Pocivavsek and Enrique Cerda for insightful discussions. This work was supported in part by the National Science Foundation MRSEC program under Grant No. DMR-0213745 and by the U.S.-Israel Binational Science Foundation.

APPENDIX

To estimate the influence of compressibility, we assume that t is the thickness of the surfactant layer. The bending modulus B varies as t^3, while the compressibility modulus K is proportional to t [43]: $B/K\simeq t^2$. The fourth-order term of bending free energy takes the form

$$b_4=\frac{5B}{4}\int_{L_0}\dot{\xi}^2\ddot{\xi}^2dx. \tag{A1}$$

In the limit of small deformation approximation, derivatives of ξ can be approximated as

$$\dot{\xi}\sim h/\lambda_c,$$

$$\ddot{\xi}\sim h/\lambda_c^2. \tag{A2}$$

Inserting Eq. (A2) into the expression of b_4, we obtain

$$b_4\sim\frac{5Bh^4L_0}{4\lambda_c^6}. \tag{A3}$$

The compression free energy takes the form

$$E_k = \frac{K}{2}\int_{L_0} \eta^2 (1+\dot{\xi}^2)^{1/2} dx, \tag{A4}$$

where K is the compressibility modulus. η is the percentage change of the length of surfactant layer. Choosing the configuration of the surfactant layer just before buckling as a reference state, we have

$$\eta = 1 - \frac{\left(\int_{L_0} (1+\dot{\xi}^2)^{1/2} dx\right)}{L_c} \simeq \frac{\Pi_{\mathrm{ex}} - \Pi_c}{K}, \tag{A5}$$

where L_c is the length of the surfactant layer just before the buckling transition. If buckling is not allowed, the compressive strain η is evidently given by the fractional decrease in L, viz. $(L_c - L_0)/L_c$. However, if buckling occurs, this strain can only decrease. As a result, the following relation holds:

$$\eta < \frac{L_c - L_0}{L_c} \sim \tilde{h}^2, \tag{A6}$$

where $\tilde{h}$ is the slope amplitude. Thus, the expansion of compression free energy in terms of $\tilde{h}$, being quadratic in η, has only a fourth-order term or higher. As a result, it does not affect the expressions of Π_c and λ_c. To the lowest order approximation, E_k can be written as

$$E_k \sim c_4 = \frac{K\eta^2 L_0}{2}. \tag{A7}$$

Comparing b_4 and c_4, we obtain a criterion of inextensibility,

$$\eta \ll \frac{t}{\lambda_c}\tilde{h}^2, \tag{A8}$$

where we have used the relation $B/K \simeq t^2$. By Eq. (A5), we have

$$\eta \simeq \frac{\Pi_{\mathrm{ex}} - \Pi_c}{K} = \frac{\Pi_{\mathrm{ex}} - \Pi_c}{A_2}\frac{A_2}{K} \sim \tilde{h}^2 A_2/K, \tag{A9}$$

where the expression of A_2 was given in Eq. (29). Inserting into the above criterion of inextensibility, we have

$$\frac{A_2}{K} \ll \frac{t}{\lambda_c}. \tag{A10}$$

As Π_{ex} approaches Π_c from above, A_2 can be approximated as

$$A_2 \simeq \frac{1}{64}\{B\phi^{(4)}(d_0)/\phi^{(2)}(d_0) - 2[B\phi^{(2)}(d_0)]^{1/2}\}$$

$$= \frac{1}{64}[B\phi^{(4)}(d_0)/\phi^{(2)}(d_0) - 8\pi^2 B/\lambda_c^2], \tag{A11}$$

where we have used the expression of λ_c in the last step. We require $A_2 > 0$ in order for the transition to be second order. Thus, the first term in Eq. (A11) must dominate the second. However, if the system were not too far away from the transition threshold between first-order buckling and second-order buckling, two terms in Eq. (A11) would have comparable order of magnitude. In such a case, we can simplify the criterion (A10) as

$$\frac{A_2}{K} \sim \frac{B}{\lambda_c^2 K} \ll \frac{t}{\lambda_c}, \quad \text{i.e.,} \quad \frac{t}{\lambda_c} \ll 1. \tag{A12}$$

The above criterion is always satisfied in the experimental systems that we are interested in. For example, suppose the monolayer thickness t is about 2 nm and the wrinkling wavelength λ_c is more than 100 nm. In such a case the approximation of inextensibility is valid. In cases of very anharmonic potentials where $\phi^{(4)}(d_0) \gg \phi^{(2)}(d_0)/\lambda_c^2$, the two terms in A_2 would not be comparable. Then the effects of compressibility could become significant.

[1] N. Bowden, S. Brittain, A. G. Evans, J. W. Hutchinson, and G. M. Whitesides, Nature (London) **393**, 146 (1998).
[2] J. Genzer and J. Groenwold, Soft Matter **2**, 310 (2006).
[3] M. Ortiz and G. Gioia, J. Mech. Phys. Solids **42**, 531 (1994).
[4] B. Audoly, Phys. Rev. Lett. **83**, 4124 (1999).
[5] E. Cerda and L. Mahadevan, Phys. Rev. Lett. **90**, 074302 (2003).
[6] Y. Pomeau and S. Rica, C. R. Acad Sci., Ser. IIa, Sci. Terre Planetes **325**, 181 (1997).
[7] A. E. H. Love, *A Treatise on the Mathematical Theory of Elasticity* (Dover, New York, 1944), Sec. 260.
[8] L. Euler, *Mechanica, Sive Motus Scientia Analytice; Expasita* (St. Petersburg, Russia, 1736).
[9] L. Pocivavsek and E. Cerda (private communication).
[10] S. T. Milner, J. F. Joanny, and P. Pincus, Europhys. Lett. **9**, 495 (1989).
[11] M. M. Lipp, K. Y. C. Lee, J. A. Zasadzinski, and A. J. Waring, Science **273**, 1196 (1996).
[12] M. M. Lipp, K. Y. C. Lee, A. J. Waring, and J. A. Zasadzinski, Biophys. J. **72**, 2783 (1997).
[13] K. E. Mueggenburg, Ph.D. thesis, University of Chicago, 2007.
[14] K. Y. C. Lee, M. M. Lipp, D. Y. Takamoto, E. Ter-Ovanesyan, J. A. Zasadzinski, and A. J. Waring, Langmuir **14**, 2567 (1998).
[15] K. L. Lam, Y. Ishitsuka, Y. Cheng, K. Chien, A. J. Waring, R. I. Lehrer, and K. Y. C. Lee, J. Phys. Chem. B **110**, 21282 (2006).
[16] G. H. Wu, Ph.D. thesis, University of Chicago, 2003.
[17] M. Tanaka and E. Sackmann, Nature (London) **437**, 656 (2005).
[18] A. S. Muresan and K. Y. C. Lee, J. Phys. Chem. B **105**, 852 (2001).
[19] E. Sackmann, Science **271**, 43 (1996).
[20] D. C. Lee, B. J. Chang, L. P. Yu, S. L. Frey, K. Y. C. Lee, S. Patchipulusu, and C. Hall, Langmuir **20**, 11297 (2004).
[21] K. D. Hobart, F. J. Kub, M. Fatemi, M. E. Twigg, P. E. Thompson, T. S. Kuan, and C. K. Inoki, J. Electron. Mater. **29**,

897 (2000).
[22] J. Liang, R. Huang, H. Yin, J. C. Sturm, K. D. Hobart, and Z. Suo, Acta Mater. **50**, 2933 (2002).
[23] R. Huang and Z. Suo, J. Appl. Phys. **91**, 1135 (2002).
[24] N. Sridhar, D. J. Srolovitz, and B. N. Cox, Acta Mater. **50**, 2547 (2002).
[25] L. Landau and E. M. Lifshitz, *Theory of Elasticity*, 3rd ed. (Pergamon, New York, 1986).
[26] P. G. de Gennes, F. Brochard, and D. Quere, *Capillarity and Wetting Phenomena* (Springer-Verlag, New York, 2003).
[27] J. Israelashvili, *Intermolecular and Surface Forces* (Academic, New York, 1985).
[28] H. Diamant, T. A. Witten, A. Gopal, and K. Y. C. Lee, Europhys. Lett. **52**, 171 (2000).
[29] W. F. Helfrich, Z. Naturforsch. C **28**, 693 (1973).
[30] J. G. Hu and R. Granek, J. Phys. II **6**, 999 (1996).
[31] R. Huang and Z. Suo, Thin Solid Films **429**, 273 (2003).
[32] A. P. Giddy, M. T. Dove, and V. Heine, J. Phys.: Condens. Matter **1**, 8327 (1989).
[33] A. Vrij and J. Th. G. Overbeek, J. Am. Chem. Soc. **90**, 3074 (1968).
[34] J. Daillant, L. Bosio, B. Harzallah, and J. J. Benattar, J. Phys. II **1**, 149 (1991).
[35] D. R. Clarke, T. M. Shaw, A. P. Philipse, and R. G. Horn, J. Am. Chem. Soc. **765**, 1201 (1993).
[36] J. S. Lyons, D. N. Furlong, and T. W. Healy, Aust. J. Chem. **34**, 1177 (1981).
[37] D. D. Lasic, *Liposomes: From Physics to Applications* (Elsevier, Amsterdam, 1993).
[38] A. Sharma, Langmuir **9**, 861 (1993).
[39] L. Lee, M. Silva, and F. Galembeck, Langmuir **19**, 6717 (2003).
[40] C. J. Van Oss, M. K. Chaudhury, and R. J. Good, Chem. Rev. (Washington, D.C.) **88**, 927 (1988).
[41] S. A. Safran, *Statistical Thermodynamics of Surfaces, Interfaces, and Membranes* (Addison-Wesley, New York, 1994).
[42] S. A. Safran, Surf. Sci. **500**, 127 (2002).
[43] U. Seifert and S. A. Langer, Europhys. Lett. **23**, 71 (1993).